Fluid–Structure Interaction of a Flexible Structure in a Turbulent Flow using LES

M. Breuer, G. De Nayer, M. Münsch

1 Introduction

A structure placed in a fluid flow is always affected by the pressure and shear forces acting on the surface leading to structural deformations or deflections. Partially these can be neglected and such a rigid body assumption strongly reduces the complexity of a numerical simulation setup. However, in many circumstances this assumption does not hold and fluid–structure interaction (FSI) becomes of major interest. Technical applications are numerous such as artificial heart valves, lightweight roofage or tents. Therefore, a need for appropriate numerical simulation tools exists for such coupled problems and this is the objective of the present study. The developments are guided by the following ideas:

- Since it is well known that the RANS approach is not an appropriate choice for the prediction of instantaneous flow processes involving large–scale flow structures (separation, reattachment, vortex shedding) very often encountered in FSI problems, large–eddy simulation (LES) is the preferred technique.
- Since LES often requires small time steps, an explicit time–marching scheme relying on a predictor–corrector method is favored. The question of how to appropriately couple this scheme with the computation of the structure dynamics had to be solved.
- Since the usage of highly specialized codes for each subtask (fluid and structure) is assumed to be advantageous, a partitioned approach is chosen where the entire FSI problem is divided into a fluid and a structure domain. The coupling between both domains has to be done via an additional coupling interface. Here aspects

M. Breuer and G. De Nayer
Professur für Strömungsmechanik (PfS), Helmut–Schmidt–Universität Hamburg, Holstenhofweg 85, D–22043 Hamburg, Germany, e-mail: breuer/denayer@hsu-hh.de

M. Münsch
Lehrstuhl für Strömungsmechanik, Universität Erlangen–Nürnberg, Cauerstr. 4, D–91058 Erlangen, Germany, e-mail: mmuensch@lstm.uni-erlangen.de

such as code-to-code communication or grid-to-grid interpolation, e.g., of loads and displacements, had to be considered.

These issues are discussed in the present contribution and then applied to a turbulent LES–FSI benchmark test case involving the flow around a flexible structure.

2 Computational Methodology

Within a FSI application the fluid forces lead to a displacement or deformation of the structure and thus the computational domain is no longer fixed but changes in time. In order to account for these variations, the most popular numerical technique is the so-called Arbitrary Lagrangian–Eulerian (ALE) formulation. Here the filtered Navier–Stokes equations for an incompressible fluid are re-formulated for a temporally varying domain on a temporally varying grid. Thus the size of the control volumes within the finite–volume scheme applied varies in time. The second–order accurate central discretization is done on a curvilinear, block-structured body–fitted grid with a collocated variable arrangement (code FASTEST–3D). To account for the subgrid scales, the classical Smagorinsky model as well as the dynamic model by Germano et al. are applied.

A challenge was to design a FSI coupling scheme, which on the one hand is appropriate for the explicit time–stepping scheme used and on the other hand avoids instabilities known from loose coupling schemes. In the scheme suggested [3, 2, 4, 7], each time step starts with an estimation of the structural displacement using a linear or quadratic extrapolation of the three preceding time steps. Within the predictor step the momentum equations are solved by an explicit time integration scheme, namely a low–storage Runge–Kutta scheme. Here the ALE formulation is taken into account, which ensures that the *space conservation law* is fulfilled. In the corrector step a Poisson equation for the pressure correction variable is solved, which guarantees a divergence–free velocity field and thus the fulfillment of the mass conservation. Whereas the predictor step is only done once per time step, the corrector step has to be repeated several times (5–10) until a predefined convergence criterion is reached. The coupling and thus the exchange of fluid forces in one direction and the resulting displacements in the other direction is conducted within the corrector step, which is repeated until a dynamic equilibrium between fluid and structure is achieved. Consequently, a strongly coupled but nevertheless still explicit time–stepping algorithm results.

Within the coupling procedure the resulting forces on the interface are computed by the finite–element CSD solver *Carat++* [5] especially developed by TU Munich for the prediction of shells or membranes. *Carat++* is based on several finite–element types and advanced solution strategies for form finding and nonlinear dynamic problems. For the dynamic analysis, different time–integration schemes such as the generalized–α method are used. In the modeling of thin-walled structures, membrane or shell elements are used for the discretization. Both, shell and membrane elements produce reduced structural models with a two–dimensional repre-

sentation which can describe the three–dimensional physical properties by introducing mechanical assumptions for the thickness direction. In our test case, the plate is modeled with a seven-parameters shell element.

Due to different discretization techniques applied for the subtasks (finite volumes vs. finite elements) also different types of grids and different grid resolutions are used leading to non–matching surface meshes. Consequently, a grid–to–grid data interpolation and transfer becomes necessary. These interpolation steps including the transfer of the fluid loads to the CSD code and the structural displacements back to the CFD code are done via the coupling interface CoMA [6] also developed by TU Munich. A conservative interpolation is used for the transfer of the fluid loads from the cell vertices of the fluid domain to the grid nodes of the structure domain (CFD→CSD), whereas a bilinear interpolation of the displacements from the structure domain to the cell vertices of the fluid domain (CSD→CFD) is applied. The grid adaptation at the interface is based on an underrelaxation of the structural response by taking an underrelaxation factor (e.g. $\alpha = 0.5$) and the displacement of the previous sub-iteration loop into account. Based on the displacement at the boundaries, the grid adjustment is presently done by a transfinite interpolation technique, but more advanced techniques such as elliptic grid smoothing to better maintain the grid quality are under investigation. Subsequent to the grid adaptation solely the corrector step of the predictor–corrector scheme is performed again and a new velocity and pressure field is obtained. Afterwards new loads for the structure solver are generated leading to an update of the corresponding displacements. The dynamic equilibrium between fluid and structure is obtained if changes of the resulting displacements within the sub-iteration cycle reaches a convergence criterion. A convergence criterion based on the loads is also under consideration. The coupling interface is based on the Message–Passing–Interface (MPI) and thus runs in parallel to the fluid and structure solver. Since MPI is also used for the parallelization of the CFD code applied, efficient coupling with respect to high–performance computing is enabled.

A variety of different test cases considering either laminar flows and/or simplified structural models assuming elastically mounted cylinders or plates have been considered to validate and evaluate the present FSI algorithm, see e.g. [3, 2, 4, 8, 7].

3 Benchmark Test Case

The present configuration leans on the benchmark case FSI3 developed within the DFG research group FOR 493 on FSI [9] for laminar flows, but is extended to the turbulent flow regime. In a channel of length $L/D = 25$ and height $H/D = 4.1$ a cylinder of diameter D is mounted. The cylinder position is slightly off–centered, with the cylinder center located at $2D$ downstream of the inflow section and with a distance of $2D$ from the lower lateral channel wall. Based on D and the constant inflow velocity U_∞ the Reynolds number of the incompressible and Newtonian fluid ($\rho^f = 1000$ kg/m^3) is set to $Re = 10^4$. In the wake of the cylinder, a flexible plate

is attached to the cylinder. The plate is of length $l = 3.5D$ and has a thickness of $h = 0.2D$. The cylinder is assumed to be fixed and rigid, whereas the material of the plate is of St. Venant–Kirchhoff type [1] characterized by a Poisson ratio of $\nu^s = 0.4$, a Young modulus of $E = 5.6 \cdot 10^6$ kg/(m s^2) and a density of $\rho^s = 1000$ kg/m^3. For the flow prediction a block–structured grid with about 17 million CVs is used. At the lateral channel boundaries a slip boundary condition is applied, whereas on the structure, no–slip boundary conditions are used. In spanwise direction periodic boundary conditions are chosen. At the channel outlet a convective outflow condition is specified. The elastic plate is resolved by the use of 10×10 four-nodes shell elements. All the nodes on the cylinder are fixed and the nodes at the free extremity are totally free. The z–displacement of the nodes on the sides are forced to be zero. Due to periodic boundary conditions set in the fluid solver there are always two nodes of the sides (one in a plane and its twin in the other plane) which have the same load. These two nodes must have the same displacement in x– and y–direction which is enforced in the CSD code.

4 Results and Discussion

For testing the entire coupling algorithm developed, the benchmark case FSI3 [9] mentioned above was considered first. With the exception of a parabolic inflow profile, the application of no–slip boundary conditions at the channel walls and a much lower Re–number of Re = 200, the setup is the same as for the LES case. For these flow predictions two different grids with either only about 27,000 or 90,000 CVs in a 2D plane were used. Exemplarily, Fig. 1(a) depicts a snapshot of the flow field by contours of the streamwise velocity in a x–y slice.

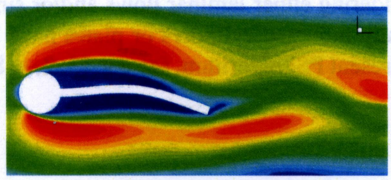

(a)

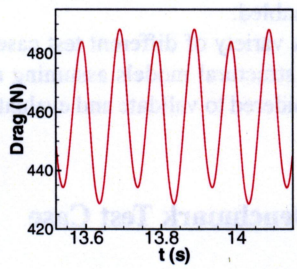

(b)

Fig. 1 Laminar flow around the flexible structure, (a) Snapshot of contours of the streamwise velocity; (b) Time history of the drag on the structure.

Despite the splitter 'plate' behind the cylinder, vortex shedding occurs. The shed vortices travel downstream and start to interact with the flexible structure leading to an oscillating structure. Fig. 1(b) shows the time history of the drag force on

the structure. After a transition phase (not shown) the amplitude of the oscillations reaches constant values. The same applies for the lift force and the displacements of point **A** located at the trailing edge on the center line of the flexible structure. The corresponding minimal and maximal values as well as the frequency of the lift force are given in Table 1 for both grids. For comparison the highly resolved finite–element simulation by Turek and Hron [9] is given. Despite some differences the overall agreement is satisfactory. Furthermore, an improvement of the results on the refined grid is visible with respect to the reference data. Partially the grid convergence seems to be small. In order to further investigate this issue, presently simulations on the next finer grid level are carried out. The coupling scheme was found to work very efficiently requiring only a few FSI iterations (5 to 7) to go below a convergence limit ensuring dynamic equilibrium, e.g. 10^{-4} for the L_2 norm of the displacements. Thus, by performing this test case the proper behavior of the whole partitioned FSI setup was proven.

Table 1 Results of the benchmark FSI3 (Re = 200) on two different grid levels.

	Resolution	Δy [$\times 10^{-3}$ m]		**Drag** [N]		**Lift** [N]		**Frequency**
		Min.	Max.	Min.	Max.	Min.	Max.	of Lift [Hz]
Coarse	27,040 CVs	-43.98	46.22	429.0	525.0	-216.0	230.0	4.99
Medium	89,952 CVs	-43.63	46.17	428.0	488.0	-166.0	210.0	5.04
Ref. [9]	highly resolved FE	-33.43	36.37	432.7	488.2	-151.4	156.4	5.46

For the turbulent case, the simulation was started with a rigid structure. The structure behind the cylinder acts like a splitter plate of length l/D = 3.5 attenuating the generation of a vortex street behind the cylinder. Fig. 2(a) depicts the pressure distribution in a x–y plane showing the shear layers with the Kelvin–Helmholtz instability leading to transition and two large vortices originating from the shedding process. The time history of the lift and drag coefficients confirms that the splitter plate does not suppress vortex shedding completely. Compared to a pure cylinder in free flow the Strouhal number decreases to about St = 0.172 which is the result of two opposing effects: splitter plate: St $\downarrow$, blockage: St $\uparrow$.

Then the plate was released and a fully coupled FSI–LES prediction was started. Owing to different loads on both sides the structure directly started to deflect in one direction, see Fig. 3(a). In this snapshot a region of low pressure is already visible at the lower side so that at a later instant the plate bent back to the initial position (Fig. 3(b)) and is then deflected in the other direction (Fig. 3(c)). To evaluate the entire deflection mode of the structure will be the task for the near future. Nevertheless, the study has shown that a reliable and efficient coupling scheme for the marriage of FSI and LES has been established.

Acknowledgements We gratefully acknowledge the cooperation with the Chair of Structural Analysis of TU Munich providing the codes Carat++ [5] and CoMA [6] including intensive support by Dipl.–Ing. Th. Gallinger, Dr.–Ing. R. Wüchner and Prof. Dr.–Ing. K.U. Bletzinger.

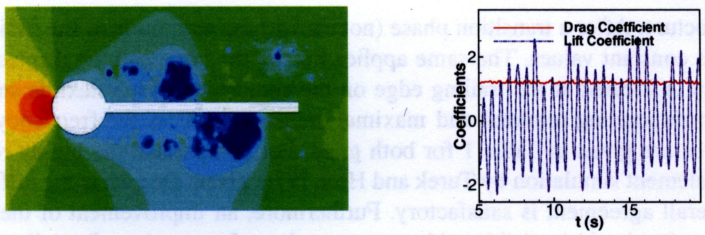

(a) (b)

Fig. 2 Turbulent flow around the rigid structure, (a) Snapshot of contours of the pressure in one x–y plane; (b) Time history of the drag and lift coefficient on the structure.

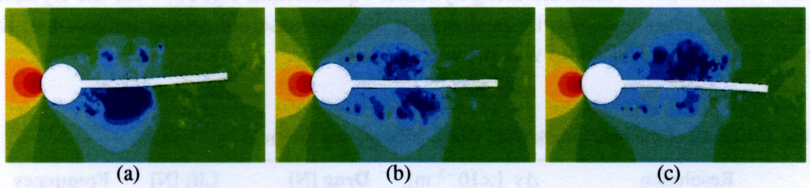

(a) (b) (c)

Fig. 3 Turbulent flow around the flexible structure, three different snapshots in time.

References

1. Belytschko, T., Liu, W.K., Moran, B.: Nonlinear Finite Elements for Continua and Structures, Wiley New York, (2000).
2. Breuer, M., Münsch, M.: LES Meets FSI – Important Numerical and Modeling Aspects, 7th Int. ERCOFTAC Workshop on DNS and LES: DLES-7, Trieste, Italy, Sept. 8–10, 2008, ERCOFTAC Series, vol. **13**, pp. 245–251, DLES VII, eds. Armenio, V. et al., Springer (2010)
3. Breuer, M., Münsch, M.: Fluid–Structure Interaction Using LES – A Partitioned Coupled Predictor–Corrector Scheme, PAMM, vol. **8**, pp. 10515–10516 (2008)
4. Breuer, M., Münsch, M.: FSI of the Turbulent Flow around a Swiveling Flat Plate Using Large-Eddy Simulation, Int. Workshop on Fluid-Structure Interaction (2008), eds. S. Hartmann et al., 31–42, Kassel University Press, ISBN 978-3-89958-666-4, Kassel (2009)
5. Fischer, M., Firl, M., Masching, H., Bletzinger, K.-U.: Optimization of Nonlinear Structures based on Object–Oriented Parallel Programming, ECT2010: Seventh Int. Conf. Engineering Computational Technology, Valencia, Spain (2010)
6. Gallinger, T., Kupzok, A., Israel, U., Bletzinger, K.-U., Wüchner, R.: A Computational Environment for Membrane–Wind Interaction. Int. Workshop on Fluid–Structure Interaction: Theory, Numerics and Applications, Herrsching, Germany, Sept. 29 – Oct. 1, (2008)
7. Münsch, M., Breuer, M.: Numerical Simulation of Fluid–Structure Interaction Using Eddy–Resolving Schemes, In: Bungartz, H.-J., Schäfer, M. (eds.) Fluid–Structure Interaction, Lecture Notes Comput. Sci. & Eng., LNCSE, Springer, Heidelberg, in press, (2010)
8. Pereira Gomes, J., Münsch, M., Breuer, M., Lienhart, H.: Flow–induced Oscillation of a Flat Plate — A Fluid–Structure Interaction Study Using Experiment and LES, 16. DGLR–Fach–Symp. STAB, RWTH Aachen, Germany, Nov. 3–5, 2008, In: Notes on Numerical Fluid Mechanics and Multidisciplinary Design, Springer, Berlin, in press, (2010)
9. Turek, S., Hron, J.: Proposal for Numerical Benchmarking of Fluid–Structure Interaction between an Elastic Object and Laminar Incompressible Flow, In: Bungartz, H.-J., Schäfer, M. (eds.) Fluid–Structure Interaction, LNCSE, vol. **53**, pp. 371–385, Springer, Heidelberg (2006)